ELSEVIER

Applied Catalysis B: Environmental 19 (1998) 103–117

APPLIED CATALYSIS B: ENVIRONMENTAL

Oxidation of sulfur dioxide to sulfur trioxide over supported vanadia catalysts

Joseph P. Dunn, Prashanth R. Koppula, Harvey G. Stenger, Israel E. Wachs*

Zettlemoyer Center for Surface Studies, Department of Chemical Engineering, Lehigh University, Bethlehem, PA 18015, USA

Accepted 2 June 1998

Abstract

The objectives of this research are to establish the fundamental kinetics and mechanism of sulfur dioxide oxidation over supported vanadia catalysts and use these insights to facilitate the design of SCR $DeNO_x$ catalysts with minimal sulfur dioxide oxidation activity. A series of supported vanadia catalysts were prepared on various metal-oxide supports: ceria, zirconia, titania, alumina and silica. Raman spectroscopy was used to determine the coordination of surface species. At low vanadia loadings, vanadia preferentially exists on oxide support surfaces as isolated tetrahedrally coordinated $(M–O)_3V^{+5}=O$ species. At higher vanadia loadings, the isolated $(M–O)_3V^{+5}=O$ species polymerize on the oxide support surface breaking two V–O–M bonds and forming two V–O–V bridging bonds.

The turnover frequency for sulfur dioxide oxidation was very low, 10^{-4} to 10^{-6} s^{-1} at 400°C, and was independent of vanadia coverage suggesting that only one vanadia site is required for the oxidation reaction. As the support was varied, sulfur dioxide oxidation activity of the supported vanadia catalysts varied by one order of magnitude (Ce>Zr, Ti>Al>Si). The basicity of the bridging V–O–M oxygen appears to be responsible for influencing the adsorption and subsequent oxidation of the acidic sulfur dioxide molecule. Over the range of conditions studied, the rate of sulfur dioxide oxidation is zero-order in oxygen, first-order in sulfur dioxide and inhibited by sulfur trioxide.

The turnover frequency for sulfur dioxide oxidation over WO_3/TiO_2 was an order of magnitude lower than that found for V_2O_5/TiO_2, and no redox synergism between the surface vanadia and tungsten oxide species was evident for a ternary $V_2O_5/WO_3/TiO_2$ catalyst. This suggests that WO_3 promoted catalysts may be suitable for low-temperature SCR where minimal sulfur dioxide oxidation activity is required.

Keywords: SCR; $DeNO_x$; Sulfur dioxide; Sulfur trioxide; Oxidation; Vanadia

1. Introduction

Sulfur dioxide (SO_2) is formed from both the oxidation of sulfur contained in fossil fuels and industrial processes that treat and produce sulfur-containing compounds. The catalytic oxidation of sulfur dioxide appears in numerous industrial processes and has a significant environmental impact because of the associated sulfur oxide (SO_x) emissions. Approximately two-thirds of the 50 billion pounds of sulfur oxides released annually in the US are emitted from coal fired power plants [1]. Industrial fuel combustion and industrial processes (primarily sulfuric acid manufacture, petroleum refining and smelting of non-ferrous metals) account for the remainder of the emissions.

*Corresponding author. Tel.: +1-610-758-4274; fax: +1-610-758-6555; e-mail: iew0@lehigh.edu

0926-3373/98/$ – see front matter
PII: S0926-3373(98)00060-5

The oxidation of sulfur dioxide to sulfur trioxide is undesirable during the selective catalytic reduction (SCR) of nitrogen oxides (NO_x) found in the flue gas of power plants. SCR removes NO_x in flue gas by reacting nitrogen oxides with ammonia and oxygen to form nitrogen and water at approximately 370°C over titania supported vanadia catalysts, e.g., V_2O_5/WO_3–MoO_3/TiO_2. Under typical SCR design and operating conditions, NO_x reduction efficiency is directly proportional to the NH_3:NO_x ratio up to NO_x reduction levels of about 80%. Ammonia readily combines with sulfur trioxide at temperatures below 250°C to form ammonium sulfates, which can block the catalyst's pores and foul downstream heat exchangers [2]. This problem is so serious that industrial specifications for SCR processes include upper limits for the outlet concentration of sulfur trioxide corresponding to approximately 1–2% sulfur dioxide conversion. Commercial SCR catalysts traditionally have low vanadia loadings due to vanadia's propensity to catalyze sulfur dioxide oxidation. A catalyst able to suppress the oxidation of sulfur dioxide to sulfur trioxide would allow lower SCR operating temperatures without the worry of ammonium sulfate production and deposition.

Two new NO_x/SO_x removal techniques, SNO_x (Haldor Topsoe) and $DeSONO_x$ (Degussa), combine SCR technology with sulfuric acid production [3,4]. Flue gas is heated to 380°C and nitrogen oxides are removed via conventional SCR technology. The products are further heated to 420°C and the sulfur dioxide is oxidized to sulfur trioxide over a V_2O_5–$K_2S_2O_7/SiO_2$ sulfuric acid contact catalyst. The sulfur trioxide is then contacted with water producing concentrated sulfuric acid. Any unreacted ammonia from the SCR reactor is oxidized to NO_x over the second catalyst bed, consequently avoiding the formation of ammonium sulfates. These and similar hybrid processes would benefit from improvements in SCR catalysts.

In spite of the industrial importance and environmental consequences of the catalytic oxidation processes involving sulfur dioxide, few fundamental studies have been performed on the kinetics and mechanism of sulfur dioxide oxidation with the exception of the unique supported liquid phase sulfuric acid contact catalyst. Under reaction conditions, i.e., at 450–610°C, the active component of sulfuric acid catalyst exists as a melt forming a very thin liquid layer on the surface of the support (only 100–1000 Å thick) and therefore, the studies on commercial sulfuric acid catalysts [5–7] are not applicable to the environmental oxidation reactions over conventional solid supported metal-oxide catalysts.

Svachula et al. [8] addressed the effects of the operating conditions (contact time, temperature), feed composition (O_2, SO_2, H_2O, NO and NH_3), and catalyst design parameters (wall thickness, vanadium content) in the oxidation of sulfur dioxide to sulfur trioxide over an industrial honeycomb $DeNO_x$ catalyst. The steady state reaction rate was found to be of fractional order in sulfur dioxide, independent of oxygen, depressed by water and ammonia and slightly enhanced by nitrogen oxides. Svachula et al. claim that the active sites for sulfur dioxide oxidation are dimeric vanadyls with sulfate ligands, identical to the active site on the molten salt sulfuric acid catalyst. However, no direct spectroscopic evidence supporting the existence of this active site was presented.

In an effort to develop a catalyst for the selective catalytic reduction of nitric oxide with ammonia with minimal sulfur dioxide oxidation activity, Morikawa et al. [9] tested several modifications of vanadia/titania catalysts for sulfur dioxide oxidation and SCR activity. Six different $M_xO_y/V_2O_5/TiO_2$ catalysts were tested, where M_xO_y=GeO_2, ZnO, Ta_2O_5, Y_2O_3, MoO_3 or WO_3. The rate of sulfur dioxide oxidation was shown to increase with increasing temperature and vanadia content. Catalysts containing tungsten oxide or molybdenum trioxide showed an increase in the activity of sulfur dioxide oxidation, while catalysts containing germanium oxide or zinc oxide showed a drastic decrease in sulfur dioxide oxidation activity. During the SCR reaction, tungsten oxide and germanium oxide modified catalysts showed an increase in NO_x reduction. In a later study Morikawa et al. [10] found the oxidation reaction to be first-order in sulfur dioxide and independent of oxygen partial pressure.

Sazonova et al. [11] tested the performance of V_2O_5/TiO_2 catalysts doped by tungsten oxide and niobium oxide for sulfur dioxide oxidation and selective catalytic reduction of nitric oxide by ammonia. The data suggests that tungsten oxide substantially decreases the oxidation of sulfur dioxide to sulfur trioxide. Niobium doped catalysts also exhibited a

slight decrease in oxidation activity. Again, increasing temperature and vanadia content increased sulfur dioxide oxidation.

Imanari et al. [12] focused on finding a high temperature SCR catalyst possessing low sulfur dioxide oxidation activity at temperatures between 400°C and 500°C. Two catalysts were tested: WO_3/Fe_2O_3 and WO_3/TiO_2. At 400°C, WO_3/Fe_2O_3 was 100 times more active for sulfur dioxide oxidation than WO_3/TiO_2. The WO_3/TiO_2 catalyst showed less than 2% conversion of sulfur dioxide over the prescribed temperature range.

The objective of this research is to establish the fundamental kinetics and mechanism of the oxidation of sulfur dioxide to sulfur trioxide over oxide catalysts that contain the oxide phase in the solid state. The oxide catalysts investigated consist of vanadia based supported metal-oxide catalysts since these are excellent model catalyst systems that also find wide application as commercial catalysts. Combining in situ molecular characterization studies with the corresponding kinetic studies have resulted in a fundamental understanding (reaction mechanism and structure–reactivity relationships) of the sulfur dioxide oxidation reaction. The new insights generated from these studies will assist in the design of SCR $DeNO_x$ catalysts with minimal sulfur dioxide oxidation activity.

2. Experimental

2.1. Preparation of supported vanadium and tungsten oxide catalysts

The oxidation catalysts used in this research program were supported metal-oxide catalysts possessing two-dimensional metal-oxide overlayers on high surface area oxide supports. A series of 1–7% V_2O_5/TiO_2 catalysts (corresponds to 0.16–1.16 monolayer coverage) were synthesized. In addition, several other supports (e.g., ceria, zirconia, alumina and silica) were impregnated with both low (1% V_2O_5, corresponding to ~2 V atoms/nm^2 for ceria and zirconia, ~0.4 V atoms/nm^2 for alumina and ~0.25 V atoms/nm^2 for silica) and monolayer (~8 V atoms/nm^2 for ceria, zirconia and alumina) loadings of vanadia. Due to weak interactions between surface vanadia species and the silica support, the highest loading impregnated onto silica was ~1 V atom/nm^2. Tungsten oxide promoted catalysts were also tested due to their extensive application in SCR catalysts [2].

Catalysts were prepared on various oxide supports: TiO_2 (Degussa P-25, 50 m^2/g); CeO_2 (Engelhard, 36 m^2/g); ZrO_2 (Degussa, 39 m^2/g); Al_2O_3 (Harshaw, 180 m^2/g) and SiO_2 (Cabot, 300 m^2/g). All of the oxide supports were washed with distilled water and isopropanol (Fisher-certified ACS, 99.9% pure), dried at 120°C for 4 h and calcined at 450°C for 2 h prior to impregnation. The supported vanadia and tungsten oxide promoted catalysts were prepared by incipient wetness impregnation. Vanadium triisopropoxide was used as the vanadium precursor. The air- and moisture-sensitive nature of the vanadium alkoxide precursor required the preparation of vanadia catalysts to be performed under a nitrogen environment using non-aqueous solutions. Solutions of known amounts of vanadium triisopropoxide (Alfa) and isopropanol, corresponding to incipient wetness impregnation volume and the final amount of vanadia required, were prepared in a glove box and dried at room temperature for 16 h. Ammonium metatungstate ($(NH_4)_6H_2W_{12}O_{40}$) was used as the tungsten precursor, however, the tungsten impregnation could be performed in air using aqueous solutions. The impregnated samples were subsequently heated at 120°C (2 h) and 300°C (2 h) in either flowing nitrogen (Linde, 99.995% pure) or oxygen (Linde, 99.99% pure) depending on the precursor. For all catalysts the final calcination was performed in oxygen at 450°C for 2 h. Table 1 lists all of the metal-oxide catalysts synthesized and their surface areas as measured by nitrogen BET (Quantasorb Model QT-3).

2.2. Raman spectrometer

Laser Raman spectra were obtained for all the catalysts to obtain molecular structural information about the surface vanadia and tungsten oxide overlayers on the oxide supports. An Ar^+ laser (Spectra Physics, Model 2020-50) tuned to 514.5 nm delivered 10–30 mW of power measured at the sample. The scattered radiation from the sample was directed into a Spex Triplemate spectrometer (Model 1877) coupled to a Princeton Applied Research (Model 1463) OMA III optical multichannel photodiode array detector. The detector was thermoelectrically cooled to −35°C to decrease the

Table 1
Composition and surface area of catalysts studied

Catalyst	V (atoms/nm^2)	V (surface coverage)	BET (m^2/g)
TiO_2	–	–	50
1% V_2O_5/TiO_2	1.3	0.17	50
2% V_2O_5/TiO_2	2.6	0.33	48
3% V_2O_5/TiO_2	3.9	0.50	48
4% V_2O_5/TiO_2	5.2	0.67	46
5% V_2O_5/TiO_2	6.5	0.83	45
6% V_2O_5/TiO_2	7.8	1.0	45
7% V_2O_5/TiO_2	9.1	1.13	41
7% WO_3/TiO_2	(7.0)[a]	(0.87)[a]	45
1% V_2O_5/7% WO_3/TiO_2	1.3 (7.0)[a]	0.17 (0.87)[a]	45
CeO_2	–	–	36
1% V_2O_5/CeO_2	2.0	0.25	36
4% V_2O_5/CeO_2	8.0	1.0	34
ZrO_2	–	–	39
1% V_2O_5/ZrO_2	2.0	0.25	38
4% V_2O_5/ZrO_2	8.0	1.0	36
Al_2O_3	–	–	180
1% V_2O_5/Al_2O_3	0.4	0.05	182
20% V_2O_5/Al_2O_3	7.3	1.0	170
SiO_2	–	–	300
1% V_2O_5/SiO_2	0.25	0.06	280
4% V_2O_5/SiO_2	1	0.25	285

[a]Corresponding value for tungsten oxide loading.

thermal noise. Twenty 30 s scans with a resolution of <2 cm^{-1} were averaged to produce the final composite spectra. Approximately 100–200 mg of the pure catalysts were made into self-supporting wafers and placed in the in situ cell. The in situ cell consists of a stationary holder, which has been described elsewhere [13]. The in situ cell was heated to 300°C for 1/2 h and then cooled to room temperature in order to dehydrate the samples before the Raman spectra were obtained. The entire procedure was performed in a stream of flowing oxygen (Linde, 99.99% pure) over the catalyst sample to ensure complete oxidation of the catalysts. The Raman spectra of the catalysts were also checked under ambient conditions to check for the effect of hydration–dehydration treatments and to discriminate between surface metal-oxide species and compound/crystallite formation.

2.3. Sulfur dioxide oxidation reaction system

Kinetic studies of sulfur dioxide oxidation were performed in a heat-traced quartz reactor system with an on-line gas-phase FTIR (Midac) capable of identifying both sulfur dioxide and sulfur trioxide and quantifying sulfur dioxide (see Fig. 1). Reaction temperature was varied between 200°C and 400°C. Varying the catalyst charge to the micro-reactor allowed space velocities to range from 10 000 to 40 000 h^{-1}, while maintaining a constant feed flowrate of 160 sccm. Sulfur dioxide and oxygen concentrations in the feed gas were varied between 40 and 2000 ppm and 0.1% and 18%, respectively. Table 2 summarizes the standard operating conditions for the sulfur dioxide oxidation kinetic experiments that were performed. Each catalyst/support system was checked for variations in steady state activity over a 120 h period. Assuming standard operating conditions, effectiveness factors were calculated to be between 0.99 and 1.00 for the catalyst particle sizes tested, i.e., 80–200 mm, indicating that heat and mass transfer limitations were not present.

2.4. Gas-phase infrared spectrometer

The gas-phase FTIR (Midac) is equipped with a 10 m path gas cell (Infrared Analysis, Model 10-PA-RC-Ag), which has a volume of 3.1 l and is operated at a pressure of 150 Torr and 25°C. In order to quantify sulfur dioxide, spectra are obtained by averaging 16 scans with a resolution of 0.5 cm^{-1}. As shown in Fig. 2(a), dilute sulfur dioxide (1000 ppm SO_2, balance He) has major IR adsorption bands in the 1300–1400 cm^{-1} range (1344, 1350, 1360 and 1372 cm^{-1}), 1100–1200 cm^{-1} range (1133 and 1164 cm^{-1}), and 480–560 cm^{-1} range (507 and 539 cm^{-1}). As seen in Fig. 2(b), sulfur trioxide (980 ppm SO_3, 20 ppm H_2SO_4, balance He) has several additional and characteristic bands at 816, 1034, 1093 and 1266 cm^{-1}.

Table 2
Standard operating conditions for kinetic studies

	Range tested	Standard condition
Reactor temperature	200–400°C	320°C
Gas hourly space velocity	10 000–40 000 h^{-1}	10 000 h^{-1}
Feed flowrate	160 sccm	160 sccm
Feed SO_2 partial pressure	40–2000 ppm	1000 ppm
Feed O_2 partial pressure	0.1–18%	18%
SO_2 conversion	0.1–99%	<10%
Catalyst particle size range	80–200 μm	80–200 μm
Catalyst charge	100–1000 mg	1000 mg

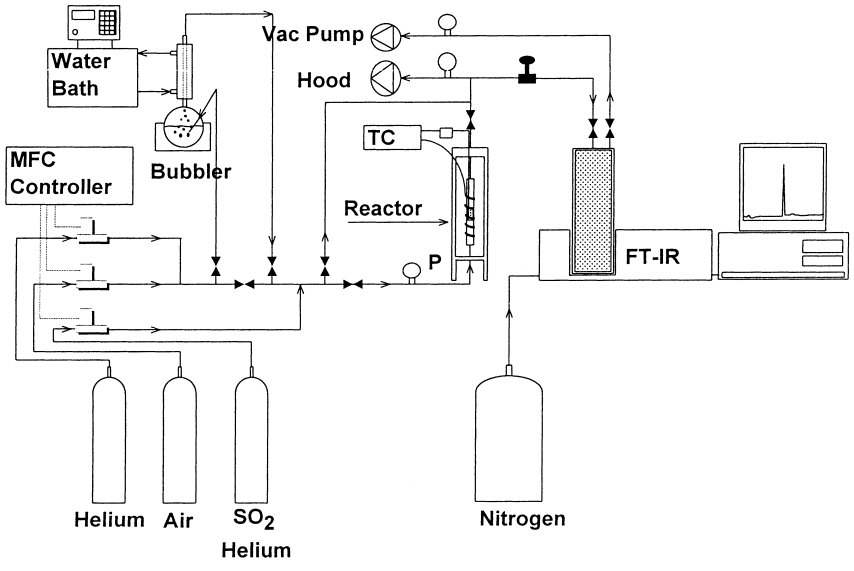

Fig. 1. Micro-reactor system used during differential kinetic studies.

The broad bands at 1600 and 3000 cm^{-1} in Fig. 2(b) are due to small (<20 ppm) quantities of sulfuric acid present in the sample. Calibration procedures are given elsewhere [14].

3. Results

3.1. Vanadia molecular structure

Previous studies have shown that depending on vanadia loading, two surface vanadia species and microcrystalline V_2O_5 particles can exist on the surface of V_2O_5/TiO_2 catalysts [15]. At low vanadia loadings, vanadia preferentially exists on the titania surface primarily as an isolated, tetrahedrally coordinated VO_4 species consisting of a single (mono-oxo) terminal V=O bond (Raman band at 1030 cm^{-1}) and three bridging vanadium–oxygen–support (V–O–M) bonds, i.e., $(M–O)_3V^{+5}=O$. At higher vanadia loadings, the isolated VO_4 species tend to polymerize on the titania surface breaking V–O–M bonds and forming V–O–V bridging bonds (Raman band at 930 cm^{-1}). At coverages exceeding a monolayer (approximately 13 mmol V^{+5}/m2 or 8 V atoms/nm^2), microcrystalline V_2O_5 particles (sharp Raman band at 994 cm^{-1}) are formed as a separate three-dimensional phase on the two-dimensional surface vanadia overlayer (i.e., the isolated and polymerized surface vanadia species). The relative concentrations of these species depend on the surface vanadia coverage as shown in Fig. 3. The weak Raman peak at approximately 790 cm^{-1} is due to the TiO_2 (anatase) support and is masked at higher vanadia loadings by the colored vanadia overlayer.

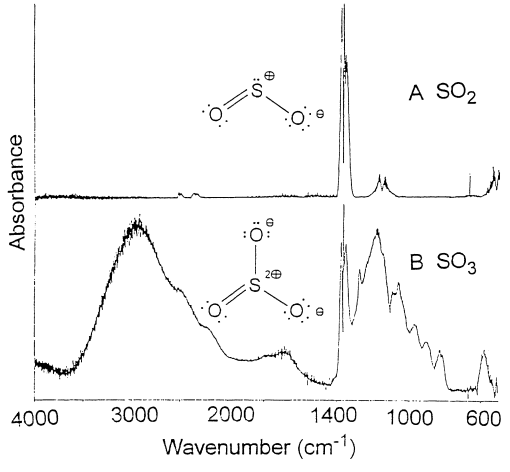

Fig. 2. Gas-phase infrared spectra of dilute sulfur dioxide and sulfur trioxide: (A) 1000 ppm SO_2, balance He; (B) 980 ppm SO_3, 20 ppm H_2SO_4, balance He.

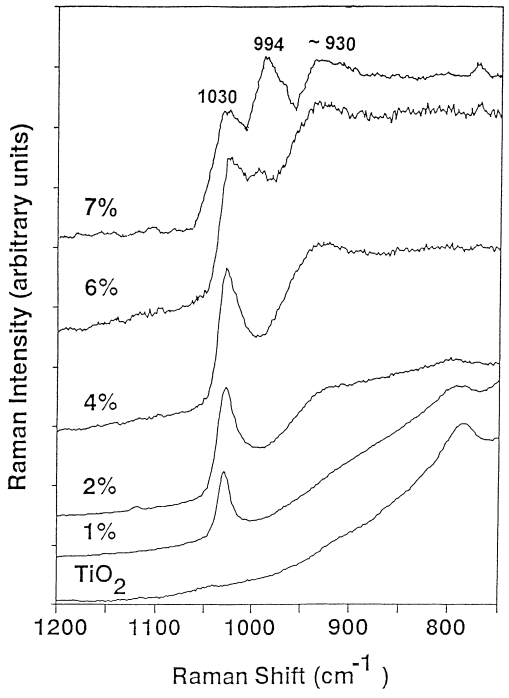

Fig. 3. Dehydrated Raman spectra of V_2O_5/TiO_2 catalysts as a function of vanadia loading.

Monolayer coverage for V_2O_5/TiO_2 corresponds to approximately 6 wt% V_2O_5, as seen in Fig. 3. A similar analysis conducted for all the supported vanadia catalyst systems yielded the following values for monolayer coverage of the surface vanadia species: 4% V_2O_5/CeO_2, 4% V_2O_5/ZrO_2, and 20% V_2O_5/Al_2O_3. A complete vanadia monolayer could not be formed on SiO_2 due to the weak interaction between the surface vanadia species and the silica support. The highest loading attained on the silica support without microcrystalline vanadium pentoxide particle formation was 4% V_2O_5/SiO_2 (approximately 1 V atom/nm^2). Furthermore, the V_2O_5/SiO_2 system is unique in possessing only isolated $(Si–O)_3V=O$ species [16]. Raman [15,17], IR [17,18] and solid state ^{51}V NMR [16] spectra of the dehydrated vanadium oxide catalysts reveal that the structures of the surface vanadium oxide species are essentially identical on ceria, zirconia, titania and alumina and possess a combination of isolated and polymerized mono-oxo VO_4 tetrahedra with similar ratios of the species at any given vanadium oxide surface coverage.

3.2. Structure of tungsten oxide promoted catalysts

Supported vanadium oxide catalysts with near monolayer coverages of tungsten oxide, as is typical of commercial SCR/DeNO$_x$ catalysts, were prepared and characterized with Raman spectroscopy. The dehydrated Raman spectrum of 1% V_2O_5/7% WO_3/TiO_2 is shown in Fig. 4 along with the spectra of 1% V_2O_5/TiO_2 and 7% WO_3/TiO_2 for reference. The Raman spectrum of 1% V_2O_5/7% WO_3/TiO_2 shows the presence of two sharp features at 1030 and 1010 cm^{-1}, and a broad Raman band at 925 cm^{-1}. The Raman spectrum of 7% WO_3/TiO_2 shows Raman features at 1010 cm^{-1} due to the symmetric stretching mode of the terminal W=O bond of mono-oxo octahedral polytungsten surface species [13]. Hence, the Raman band at 1010 cm^{-1} for the 1% V_2O_5/7% WO_3/TiO_2 sample is due to the W=O vibration, and the remaining bands at 1030 and 925 cm^{-1} are due to the vanadium–oxygen vibrations discussed above. The addition of high loadings of tungsten oxide has only slightly perturbed the surface vanadia species. A shift

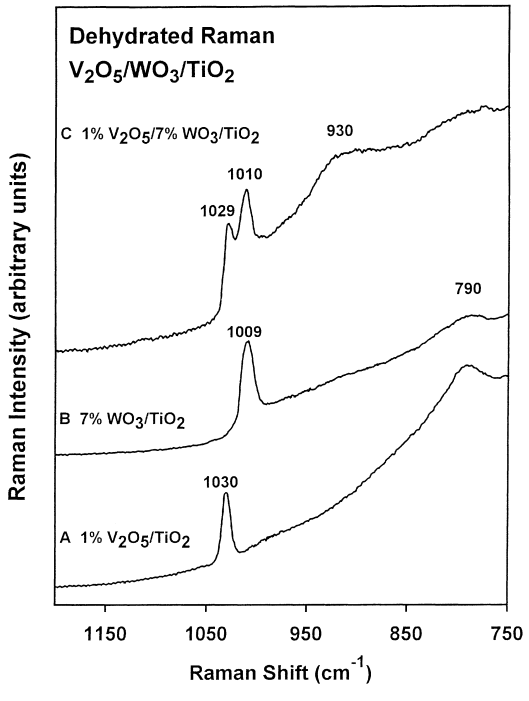

Fig. 4. Dehydrated Raman spectra of 7% WO_3/TiO_2, 1% V_2O_5/TiO_2 and 1% V_2O_5/7% WO_3/TiO_2.

of the 1027 cm^{-1} Raman band to 1030 cm^{-1} is observed and the ratio of the 925–1030 cm^{-1} signal has increased, corresponding to an increase in the ratio of the polymerized to isolated surface VO_4 species. No evidence of the formation of tungsten oxide–vanadium oxide compounds was found. No features of microcrystalline V_2O_5 or WO_3 particles are observed for the 1% V_2O_5/7% WO_3/TiO_2 sample. Monolayer loadings of the WO_3/TiO_2 system correspond to approximately 8% WO_3.

3.3. Effect of surface vanadia coverage on sulfur dioxide oxidation activity

The sulfur dioxide oxidation activity of V_2O_5/TiO_2 catalysts of variable loading (1–6% V_2O_5) was determined between 200°C and 400°C. At these loadings, Raman spectroscopy has confirmed the presence of only molecularly dispersed vanadia species on the catalyst support and, consequently, the sulfur dioxide oxidation activity can be normalized per surface vanadium atom (the turnover frequency – TOF). Normalizing the reaction rate with respect to vanadium atoms inherently assumes that all the surface vanadium oxide species participate equally in the reaction. The turnover frequency of the V_2O_5/TiO_2 catalysts (expressed in units of molecules of sulfur dioxide oxidized per surface vanadium oxide site per second) is plotted as a function of vanadia loading in Fig. 5.

The magnitude of the turnover frequency for 1% V_2O_5/TiO_2 varied from 3×10^{-6} s^{-1} at 200°C to 1×10^{-4} s^{-1} at 400°C. In addition, the results show that the turnover frequency is approximately constant as vanadia loading is varied. Therefore, the reactivity of titania supported vanadium oxide catalysts for the oxidation of sulfur dioxide to sulfur trioxide is (1) independent of changes in the local environment (i.e., increasing density of surface VO_4 species at higher loadings with a corresponding increase in bridging V–O–V bond formation) of the surface vanadium oxide species and (2) requires the presence of only a single surface vanadium oxide site for the reaction to proceed.

3.4. Effect of support on sulfur dioxide oxidation activity

The specific oxide support (e.g., ceria, zirconia, titania, alumina and silica) was varied to determine to what extent the oxide support influences the redox properties of the surface vanadia overlayer. Variation in turnover frequency with the specific oxide support will reflect on the contribution of vanadium–oxygen–support (V–O–M) bonds in the oxygen insertion reaction. At the highest temperature studied, i.e., 400°C, the bare metal-oxide supports showed negligible sulfur dioxide oxidation activity. As seen in Fig. 6, the turnover frequencies for sulfur dioxide oxidation over

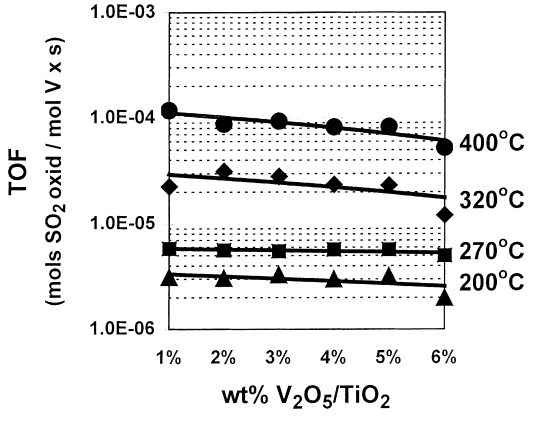

Fig. 5. Sulfur dioxide oxidation turnover frequency (TOF) of V_2O_5/TiO_2 catalysts as a function of vanadia loading and reaction temperature. Standard operating conditions listed in Table 2 followed.

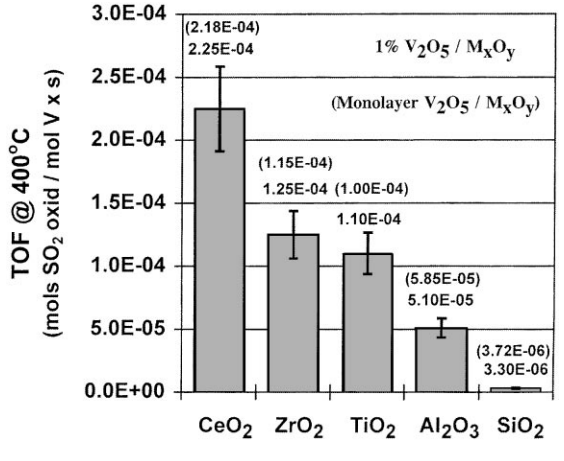

Fig. 6. Sulfur dioxide oxidation turnover frequency (TOF) of 1% and monolayer V_2O_5 impregnated on various supports. Reaction temperature=400°C, otherwise standard operating conditions listed in Table 2 followed.

1% V_2O_5 catalysts follow the trend: $V_2O_5/CeO_2 > V_2O_5/ZrO_2$, $V_2O_5/TiO_2 > V_2O_5/Al2O_3 > V_2O_5/SiO_2$. In addition, monolayer supported vanadium oxide catalysts displayed essentially the same sulfur dioxide oxidation turnover frequencies. However, deactivation of 4% V_2O_5/CeO_2, attributed to the formation of cerium vanadate (major Raman band at 800 cm^{-1}), occurred after 4 h on-line. Monolayer V_2O_5/ZrO_2 and V_2O_5/TiO_2 showed a 10% decrease in sulfur dioxide oxidation activity after 12 h on-line. BET and Raman analyses of the monolayer V_2O_5/ZrO_2 and V_2O_5/TiO_2 after reaction at 400°C revealed a 5–10% decrease in catalyst surface area and the formation of trace amounts of V_2O_5 crystals on the two-dimensional surface vanadia overlayer.

Hardcastle et al. [19] showed that the Raman frequency of a vanadium–oxygen bond is related to its bond strength. From this relationship the Raman frequencies of the terminal V=O bonds of the various supported vanadium oxide catalysts employed in this study are converted to bond strengths and plotted versus the respective sulfur dioxide oxidation turnover frequencies in Fig. 7. It is evident from Fig. 7 that no relationship exists between the terminal V=O bond strength and reactivity in the sulfur dioxide oxidation reaction. Thus, the reactivity of the supported vanadium oxide catalysts is not related to the strength of the terminal V=O bond or, as stated previously, the presence or absence of V–O–V bridging bonds and

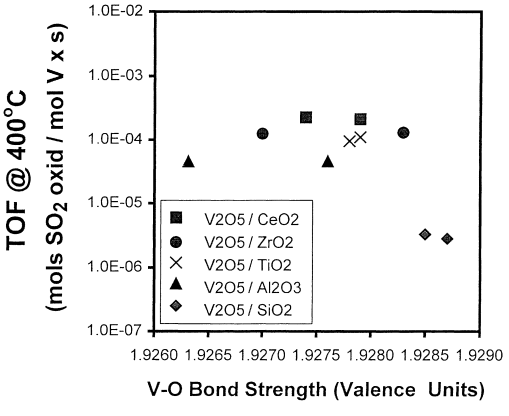

Fig. 7. Variation of sulfur dioxide turnover frequency with V=O bond strength for supported vanadium oxide catalysts. Bond strength of V=O terminal bond calculated from Raman band positions using [23].

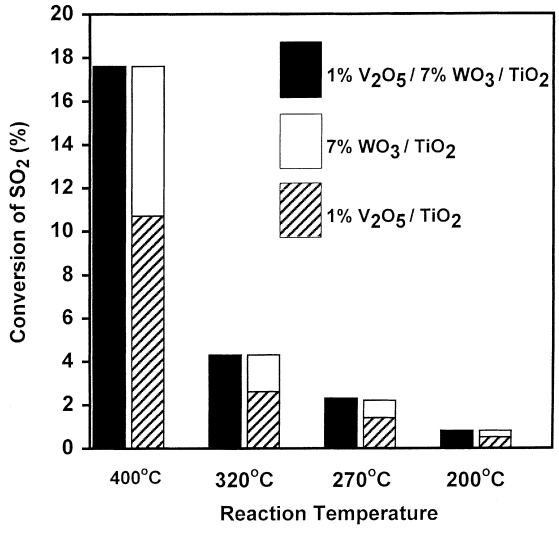

Fig. 8. Sulfur dioxide oxidation activity of: (□) 7% WO_3/TiO_2; (▨) 1% V_2O_5/TiO_2 and (■) 1% V_2O_5/7% WO_3/TiO_2. Standard operating conditions listed in Table 2 followed.

consequently, must be related to the bridging vanadium–oxygen–support (V–O–M) bond.

3.5. Reactivity of tungsten oxide promoted catalysts

As shown in Fig. 8 1% V_2O_5/7% WO_3/TiO_2 was 70% more active for sulfur dioxide oxidation than unpromoted 1% V_2O_5/TiO_2 between 200°C and 400°C. The turnover frequency for sulfur dioxide oxidation over WO_3/TiO_2 (TOF_W) was an order of magnitude lower than that found for V_2O_5/TiO_2 (TOF_V): 1×10^{-5} molecules of sulfur dioxide oxidized per surface tungsten oxide site per second versus 1×10^{-4} molecules of sulfur dioxide oxidized per surface vanadium oxide site per second at 400°C. The magnitude of the increase in the rate of sulfur dioxide oxidation exhibited by 1% V_2O_5/7% WO_3/TiO_2 relative to 1% V_2O_5/TiO_2 was identical to the rate of sulfur dioxide oxidation over 7% WO_3/TiO_2, indicating that surface vanadia and tungsten oxide species are acting independently without synergistic interactions.

3.6. Influence of feed gas compositions on oxidation reaction rate

The effect of oxygen partial pressure on the oxidation of sulfur dioxide over 1% to 6% V_2O_5/TiO_2 is

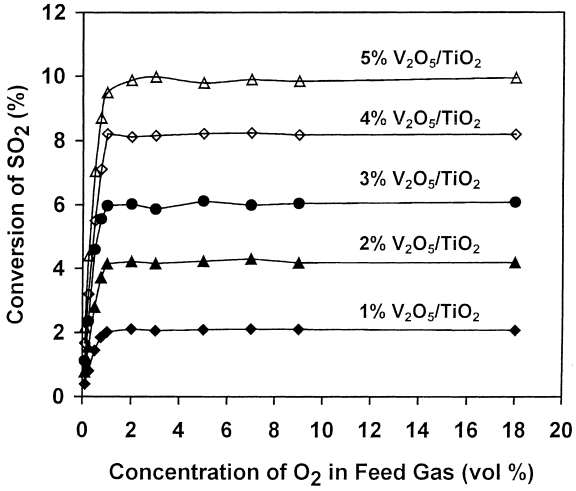

Fig. 9. Sulfur dioxide oxidation activity as a function of oxygen partial pressure for 1–6% V_2O_5/TiO_2 catalysts. Standard operating conditions listed in Table 2 followed.

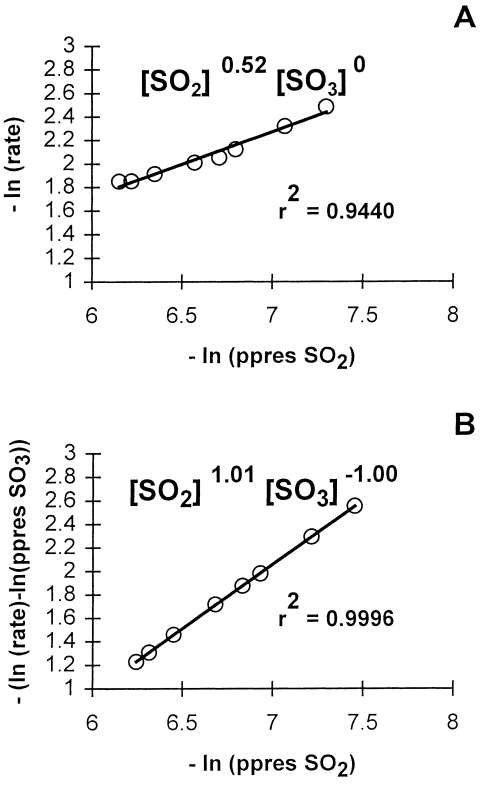

Fig. 10. Sulfur dioxide oxidation rate dependency on feed sulfur dioxide partial pressure: (A) assuming no sulfur trioxide adsorption; (B) assuming competitive adsorption between sulfur dioxide and sulfur trioxide on active vanadia species. Standard operating conditions listed in Table 2 followed.

represented in Fig. 9. For oxygen partial pressures above 1 vol% oxygen, the rate of oxidation was nearly constant indicating that the rate is independent (i.e., 0.02 ± 0.04 order) of the gas-phase oxygen partial pressure. When the oxygen partial pressure was varied between 0.1 and 1 vol% oxygen, the dependence of the rate of oxidation on the gas-phase oxygen partial pressure was seen to be approximately half order (i.e., 0.53 order). Thus, in the case of industrial conditions traditionally experienced by supported vanadium oxide catalysts (e.g., 2–6 vol% oxygen), the catalyst surface is essentially saturated with adsorbed oxygen, and consequently, the rate of reaction will show a zero-order dependence on the gas-phase oxygen partial pressure.

The influence of sulfur dioxide partial pressure on the rate of oxidation requires a more complex analysis due to the presence of the product sulfur trioxide, which competes with sulfur dioxide for adsorption on the surface vanadia species. As shown in Fig. 10(a), when product inhibition by sulfur trioxide is not taken into account, the apparent reaction rate dependence on gas-phase sulfur dioxide concentration for a 1% V_2O_5/TiO_2 catalyst can be crudely fitted to a 0.52 ± 0.09 order dependence. As shown in Fig. 10(b), assuming competitive adsorption of sulfur trioxide, the rate dependence on sulfur dioxide concentration appears to be 1.01 ± 0.03 order with a -1.00 ± 0.03 order dependence on sulfur trioxide. Similar to our findings for sulfur dioxide oxidation, Holstein and Machiels [20] investigated the phenomenon of competitive adsorption of reaction products in the selective oxidation of methanol to formaldehyde and discussed extensively how reaction orders and apparent activation energies will be underestimated when product concentration is not included in the power law rate expression for reaction systems strongly inhibited by products. Repeating this analysis for the catalysts listed in Table 3 produced comparable values for the reaction orders for sulfur dioxide and sulfur trioxide. This leads to the following power law rate expression for sulfur dioxide oxidation over solid supported vanadium oxide catalysts under typical industrial conditions:

Table 3
Power law rate expression constants and apparent activation energies for sulfur dioxide oxidation over supported vanadia catalysts

Catalyst	$[SO_2]^x$ (50–2000 ppm)	$[O_2]^y$ (1–18%)	$[O_2]^y$ (0.1–1.0%)	$[SO_3]^z$ (0–1000 ppm)	E_a (kcal/mol) 200–400°C
1% V_2O_5/TiO_2	1.01±0.03	0.02±0.03	0.53±0.14	−1.00±0.03	19.7±1.6
2% V_2O_5/TiO_2	1.02	−0.01	0.61	−0.99	19.7
3% V_2O_5/TiO_2	0.99	0.01	0.48	−0.98	20.3
4% V_2O_5/TiO_2	1.01	0.03	0.62	−1.02	20.6
5% V_2O_5/TiO_2	1.01	−0.01	0.52	−1.00	22.1
6% V_2O_5/TiO_2	1.06	−0.02	0.46	−0.96	22.4
1% V_2O_5/CeO_2	1.02	0.03	0.70	−1.00	22.2
1% V_2O_5/ZrO_2	0.97	0.02	0.55	−1.00	22.1
1% V_2O_5/Al_2O_3	0.97	0.02	0.49	−1.04	18.7

$$r_{SO_2} = \frac{k[SO_2]^{1.01\pm0.03}[O_2]^{0.02\pm0.04}}{[SO_3]^{1.00\pm0.03}}. \quad (1)$$

Apparent activation energies over the 200–400°C range 20.5±1.5 kcal/mol were calculated from this expression for the catalysts listed in Table 3.

4. Discussion

At low vanadia loadings, vanadia preferentially exists on oxide support surfaces as isolated tetrahedrally coordinated $(M–O)_3V^{+5}=O$ species. At higher vanadia loadings, the isolated $(M–O)_3V^{+5}=O$ species tend to polymerize on the oxide support surface breaking V–O–M bonds and forming V–O–V bridging bonds. The sulfur dioxide oxidation reactivity of supported vanadium oxide catalysts is not related to either the strength of the terminal V=O bond or the presence or absence of V–O–V bridging bonds. The finding that the sulfur dioxide oxidation turnover frequency is independent of the density of surface vanadia species was first reported by Morikawa et al. [9] and confirmed in the present study. This suggests that only one surface vanadia site is involved in the reaction. This observation is in contrast to the mechanism of sulfur dioxide oxidation over $V_2O_5/WO_3/TiO_2$ proposed by Forzatti and co-workers [8], which assumes a dimeric vanadyl species as the active site.

The sulfur dioxide oxidation reactivity is apparently related to the bridging V–O–M bond since changing the specific oxide support ligand alters the turnover frequency by an order of magnitude. The only significant differences between the surface vanadia species on the various oxide supports are the oxide support ligands (e.g., Ce, Zr, Ti, Al or Si). The electronegativity of the oxide support cation affects the electron density on the bridging V–O–M oxygen: a lower cation electronegativity will result in a slightly higher electron density (more basic V–O–M oxygen) and a higher cation electronegativity will result in a slightly lower electron density (less basic V–O–M oxygen). Comparison of the Sanderson electronegativities of the oxide support cations (Ce=0.72<Zr=0.90<Ti=1.50<Al=1.71<Si=2.14) [21] with the sulfur dioxide oxidation turnover frequencies shown in Fig. 6 (Ce>Zr, Ti>Al>Si) reveals an inverse correlation: the lower the oxide support cation electronegativity the higher the sulfur dioxide oxidation turnover frequency. Therefore, the more basic the bridging V–O–M bond the higher the activity towards adsorption and subsequent oxidation of the acidic sulfur dioxide molecule. Conversely, a less basic bridging oxygen depresses the adsorption of sulfur dioxide. Thus, it appears that the catalysts exhibiting higher turnover frequencies contain a higher percentage of vanadia sites capable of adsorbing sulfur dioxide and subsequently undergoing redox cycles under reaction conditions.

Similarly, this analysis may be applied to other catalytic oxidation reactions over supported vanadia catalysts. The mechanism and kinetics of methanol oxidation to formaldehyde over vanadia catalysts has been extensively examined in recent years [22]. It has been proposed that methanol adsorbs at a bridging vanadium–oxygen–support (V–O–M) bond via protonation of the bridging oxygen (H–O–M) and formation of a methoxy ($V–OCH_3$) intermediate. The rate

determining step is the subsequent breaking of a methyl C–H bond to form formaldehyde. The high turnover frequencies for methanol oxidation at 230°C over monolayer vanadia catalysts (i.e., V_2O_5/CeO_2 ($101\ s^{-1}$), V_2O_5/ZrO_2 and V_2O_5/TiO_2 ($100\ s^{-1}$), $V_2O_5/Nb2O_5$ ($10^{-1}\ s^{-1}$), $V_2O_5/Al2O_3$ ($10^{-2}\ s^{-1}$), and V_2O_5/SiO_2 ($10^{-4}\ s^{-1}$)) may be related to high concentrations of surface methoxy species present under reaction conditions [23]. In agreement with this, initial results from in situ IR studies of monolayer vanadia catalysts show that, while under methanol oxidation reaction conditions at steady state, methoxy species densely populate the catalyst surface. Furthermore, the trend in turnover frequencies for oxidation of the mildly acidic methanol molecule (V/Ce>V/Zr, V/Ti>V/Nb>V/Al>V/Si) follows the same pattern as that observed for sulfur dioxide oxidation and inversely correlates with the Sanderson electronegativities.

The reason for the extremely low sulfur dioxide oxidation turnover frequencies exhibited by monolayer vanadia catalysts ($3.7\times10^{-6}\ s^{-1}$ for V_2O_5/SiO_2 to $2.2\times10^{-4}\ s^{-1}$ for V_2O_5/CeO_2 at 400°C) may be either that: (1) the quantity of vanadium oxide–sulfur oxide surface complexes formed under reaction conditions is very low, however, once formed the surface complexes readily produce sulfur trioxide (low adsorption probability, fast reaction); (2) large numbers of stable surface complexes are formed, which slowly react to produce sulfur trioxide (high adsorption probability, slow reaction) or (3) small numbers of stable surface complexes are formed (low adsorption probability, slow reaction). As long as the surface coverage of adsorbed sulfur dioxide is not so high as to be limited by steric factors, the number of vanadium oxide–sulfur oxide surface complexes formed at a certain temperature, as determined by adsorption experiments, can be viewed as the maximum number of vanadia sites capable of undergoing redox cycles at that temperature. Kijlstra et al. [24] observed that following oxidative adsorption of sulfur dioxide at 175°C on a monolayer V_2O_5/TiO_2 ($\sim$13 mmol $V^{+5}\ M^2$; $\sim$8 V atoms/nm^2) catalyst the uptake of sulfur dioxide corresponded to <0.05 mmol SO_2/m^2; fewer than 0.4% of the surface vanadium sites adsorbed a sulfur dioxide molecule. Le Bars et al. [25] employed sulfur dioxide as a probe for basic sites present on V_2O_5/Al_2O_3 catalysts at 80°C. As vanadia surface coverage approached a monolayer the volumetric uptake of sulfur dioxide fell below the limit of detection (<0.09 mmol SO_2/m^2) of the adsorption chamber used in the study. In addition, dehydrated IR and Raman studies of sulfate promoted monolayer vanadia catalysts (e.g., V_2O_5/TiO_2 [26,27], V_2O_5/CeO_2 [27], V_2O_5/ZrO_2 [27] and $V_2O_5/Al2O_3$ [27]) fail to detect spectral bands characteristic of a vanadium oxide–sulfur oxide surface complexes. Thus, consistent with options (1) and (3) above, it appears that the low sulfur dioxide oxidation turnover frequencies of monolayer vanadia catalysts may be due to a lack of vanadia surface sites adsorbing sulfur dioxide and undergoing redox cycles under reaction conditions (low adsorption probability). Since no data regarding the fundamental rate of vanadium oxide–sulfur oxide surface complex decomposition to products is currently found in the literature, it is not possible to distinguish between the two options.

The failure to detect appreciable amounts of vanadium oxide–sulfur oxide surface complexes under reaction conditions obscures the exact molecular structure of this complex. It is possible to hypothesize two distinct structures for the vanadium oxide–sulfur oxide surface complexes: $SO_{2(g)}$ can adsorb and coordinate onto the vanadium–oxygen–support (V–O–M) bond resulting in either the $(V^{+5})\cdot SO_2$-ads or the $(V^{+3})\cdot SO_3$-ads state. This structural ambiguity allows two different reaction pathways to be proposed. As shown in Fig. 11, the mechanism of sulfur dioxide oxidation over supported vanadia catalysts involves the adsorption and coordination of $SO_{2(g)}$ onto the vanadium–oxygen–support (V–O–M) bond of either isolated or polymerized surface $(M–O)_3V^{+5}=O$ tetrahedra:

$$\text{rxn 1.}\quad SO_2 + (V^{+5}) \overset{K_1}{\leftrightarrow} (V^{+5})\cdot SO_2\text{-ads or } (V^{+3})\cdot SO_3\text{-ads} \tag{2}$$

The sulfur dioxide adsorption is followed by the slow cleavage of the V^{+5}–O–SO_2 bond and formation of SO_3(g), which represents the rate determining step

$$\text{rxn 2. (rds)}\quad (V^{+5})\cdot SO_2\text{-ads or } (V^{+4})\cdot SO_3\text{-ads} \overset{k_2}{\rightarrow} SO_3 + (V^{+3}) \tag{3}$$

The coordination of the surface (V^{+3}) site is presently unresolved in the literature [15].

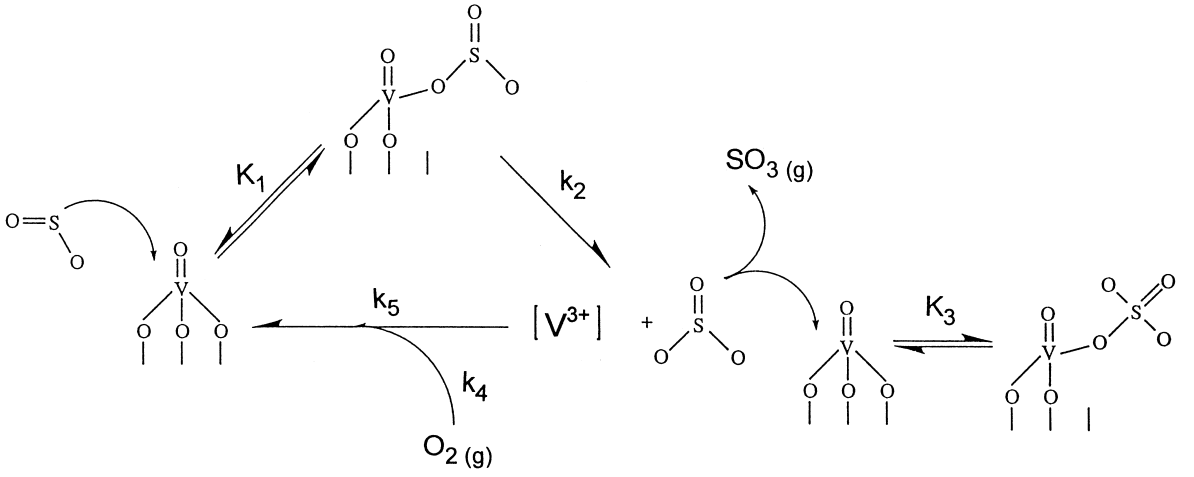

Fig. 11. Proposed mechanism for sulfur dioxide oxidation over solid vanadia catalysts. Reaction pathway may involve either a $(V^{+5})\cdot SO_2$-ads (shown) or $(V^{+3})\cdot SO_3$-ads intermediate complex.

As discussed above, the basicity of the bridging oxygen in the V–O–M bond appears to be responsible for influencing the adsorption of acidic molecules on the surface vanadia species. The electronic structures of sulfur dioxide and sulfur trioxide molecules in the gas-phase, shown in Fig. 2, indicate the electron deficiency of the sulfur atom. The electron deficiency and consequently, the acidity of the sulfur in the resonance hybrid structure for sulfur trioxide (+2) is higher than that for sulfur dioxide (+1). As a result, sulfur trioxide will experience a greater attraction to the electrons of the bridging oxygen of the V–O–M bond, resulting in a preferential adsorption of sulfur trioxide. This results in a stronger bonding of sulfur trioxide to the surface vanadia species and, consequently, competitive adsorption on (V^{+5}) sites:

$$\text{rxn 3.}\quad SO_3 + (V^{+5}) \overset{K_3}{\leftrightarrow} (V^{+5})\cdot SO_3\text{-ads} \tag{4}$$

Assuming that the two competing adsorption processes are each in equilibrium yields

$$[(V^{+5})\cdot SO_2\text{-ads}] = K_1 P_{SO_2}[(V^{+5})] \tag{5}$$

and

$$[(V^{+5})\cdot SO_3\text{-ads}] = K_3 P_{SO_3}[(V^{+5})] \tag{6}$$

The reduced (V^{+3}) site is then reoxidized by dissociatively adsorbed oxygen, thereby regenerating the active (V^{+5}) sites:

$$\text{rxn 4.}\quad O_2 \overset{K_4}{\leftrightarrow} 2\text{O-ads} \tag{7}$$

$$\text{rxn 5.}\quad \text{O-ads} + (V^{+3}) \overset{k_5}{\rightarrow} (V^{+5}) \tag{8}$$

The concentration of the dissociatively adsorbed oxygen species is given by:

$$[\text{O-ads}] = (K_4 P_{O_2})^{1/2}. \tag{9}$$

Assuming pseudo-steady state, the overall reaction rate is that of the rate limiting step (Eq. (3), rxn 2). The rate of the reaction involving the simultaneous regeneration of the active (V^{+5}) species and disappearance of reduced (V^{+3}) species (Eq. (8), rxn 5) will, therefore, be limited by the rate of the rate limiting step. At steady state, the rates of disappearance and generation of (V^{+3}) are equal. This is consistent with the Mars–van Krevelen redox mechanism and allows the rate of the overall reaction to be expressed as

$$r = r_2 = r_5 = k_2[(V^{+5})\cdot SO_2 - \text{ads}] \text{ or}$$
$$k_2[(V^{+3})\cdot SO_3\text{-ads}] = k_5[\text{O-ads}][(V^{+3})], \tag{10}$$

which upon rearrangement gives

$$[(V^{+3})] = (k_2 K_1 / k_5 K_4^{1/2}) P_{SO_2} P_{O_2}^{-1/2}[(V^{+5})]. \tag{11}$$

Writing a total site balance for the active sites leads to

$$[L] = [(V^{+5})] + [(V^{+3})] + [(V^{+5}) \cdot SO_2\text{-ads}] + [(V^{+5}) \cdot SO_3\text{-ads}] \text{ or } [L] = [(V^{+5})] + [(V^{+3})] + [(V^{+3}) \cdot SO_3\text{-ads}] + [(V^{+5}) \cdot SO_3\text{-ads}], \quad (12)$$

where $[L]$ is the total initial concentration of the (V^{+5}) sites.

Substituting Eqs. (5), (6) and (11) into Eq. (12) gives

$$[(V^{+5})] = \frac{[L]}{1 + (k_2K_1/k_5K_4^{1/2})(P_{SO_2}/P_{O_2}^{1/2}) + K_1P_{SO_2} + K_3P_{SO_3}}, \quad (13)$$

which is related to $[(V^{+4})]$ through Eq. (11)

$$[(V^{+3})] = \frac{(k_2K_1/k_5K_4^{1/2})[L]P_{SO_2}}{P_{O_2}^{1/2} + (k_2K_1/k_5K_4^{1/2})P_{SO_2} + K_1P_{SO_2}P_{O_2}^{1/2} + K_3P_{SO_3}P_{O_2}^{1/2}}. \quad (14)$$

Substituting Eqs. (9) and (14) into Eq. (10) and simplifying provides an expression for the overall rate

$$r = \frac{(k_2K_1)[L]P_{SO_2}P_{O_2}^{1/2}}{(k_2K_1/k_5K_4^{1/2})P_{SO_2} + (1 + K_1P_{SO_2} + K_3P_{SO_3})P_{O_2}^{1/2}}. \quad (15)$$

For the case of high oxygen gas-phase partial pressures, as used in the experimental conditions, the above expression further reduces to

$$r = \frac{(k_2K_1)[L]P_{SO_2}P_{O_2}^0}{1 + K_1P_{SO_2} + K_3P_{SO_3}}. \quad (16)$$

In accordance with the above discussion, the observation that the adsorption of sulfur dioxide onto surface vanadia species is inefficient leads to a low value of K_1. Furthermore, as seen from the discussion on product inhibition, sulfur trioxide is preferentially adsorbed on the active sites resulting in $K_3 \gg K_1$, and therefore the sulfur dioxide term in the denominator can be neglected. Thus, the final rate expression is given by

$$r = \frac{(k_2K_1[L]/K_3)P_{SO_2}P_{O_2}^0}{P_{SO_2}} \quad \text{or} \quad r = \frac{k'[SO_2][O_2]^0}{[SO_3]}, \quad (17)$$

which compares well with the expression derived from the experimental results

$$r_{SO_2} = \frac{k[SO_2]^{1.01\pm0.03}[O_2]^{0.02\pm0.04}}{[SO_3]^{1.00\pm0.03}}. \quad (18)$$

This rate expression is somewhat similar to previously reported kinetic expressions for sulfur dioxide oxidation over traditional, non-molten-salt, vanadia based catalysts. The observation that the sulfur dioxide oxidation reaction rate is independent of oxygen partial pressure above 0.5–1.0 vol% is in agreement with the results reported by Svachula et al. [8] and Morikawa et al. [10]. Svachula et al. found that sulfur dioxide oxidation over similar catalysts at 330°C exhibited a decreasing fractional order dependence on sulfur dioxide concentration in the range 200–1500 ppm. The results of Svachula et al. can be explained with the aid of Fig. 10(a). When the kinetic rate expression is written without a term accounting for the inhibition of sulfur trioxide, the rate appears to be approximately half-order in sulfur dioxide concentration over the 45–2000 ppm range and does exhibit a decreasing fractional order dependence as sulfur dioxide concentration increases (e.g., 0.56 reaction order over the 45–500 ppm SO_2 range and 0.49 reaction order over the 500–2000 ppm SO_2 range).

Morikawa et al. [10] report that the rate of sulfur dioxide oxidation over V_2O_5/TiO_2 exhibits a first-order dependence on the sulfur dioxide partial pressure and is independent of sulfur trioxide at temperatures between 400°C and 550°C. This is not necessarily inconsistent with the mechanism and kinetic expression proposed above (Eq. (16)). For the reversible exothermic adsorption of sulfur dioxide and sulfur trioxide onto surface vanadia species, as the temperature is increased the adsorption equilibrium constants decrease, which may result in the magnitudes of $(K_1P_{SO_2})$ and $(K_3P_{SO_3})$ being negligible compared to one in the denominator of Eq. (16). The resulting kinetic expression would indeed be first-order in sulfur dioxide partial pressure and independent of sulfur trioxide.

Kinetic and Raman studies of catalysts with near monolayer coverages of tungsten oxide impregnated onto both bare titania supports and 1% V_2O_5/TiO_2 catalysts demonstrated that there are no synergistic interactions, toward either promoting or suppressing

sulfur dioxide oxidation, occurring between the surface vanadia and tungsten oxide overlayers. The opposite conclusion was drawn by Sazonova et al. [11] who report that addition of high loadings of tungsten oxide to a V_2O_5/TiO_2 catalyst substantially suppresses sulfur dioxide oxidation activity. However, Sazonova et al. failed to recognize that for the loadings of surface vanadia (~3 monolayers) and tungsten oxide (~6 monolayers) species used in their study, the surface species are no longer molecularly dispersed but form WO_3 and V_2O_5 crystallites. Since no information about the structure or dispersion of the metal oxides was presented, it is not possible to clearly identify the reason for the decrease in oxidation activity, but is most likely due to the presence of crystalline phases.

It has been proposed by Lietti et al. [28] that electronic interactions between neighboring surface vanadia and tungsten oxide sites on a titania support may lead to an increase in both SCR $DeNO_x$ and sulfur dioxide oxidation activities at temperatures below 230°C. This is based on the fact the reactivity of a ternary (i.e., 1.4% V_2O_5/9% WO_3/TiO_2) catalyst in the SCR reaction is higher than that of the corresponding binary (i.e., 1.4% V_2O_5/TiO_2 and 9% WO_3/TiO_2) catalysts physically combined. Lietti et al. acknowledge that at temperatures above 230°C this synergism is due to both the increased Brønsted acidity [29–33] of the ternary catalyst and higher surface vanadia and tungsten oxide surface coverages on the titania support [32,33], which allows the dual-site mechanism of the SCR reaction to proceed more efficiently. However, at temperatures below 230°C they propose that (1) the SCR rate determining step is the reoxidation of the reduced surface vanadia species and (2) the ternary catalyst possesses superior redox properties at these temperatures. The redox properties of ternary $V_2O_5/WO_3/TiO_2$ catalysts at 200°C and 230°C have been probed by the single-site sulfur dioxide oxidation and selective oxidation of methanol to formaldehyde [34] reactions, respectively. However, neither study showed an increase in redox activity for the ternary catalyst with respect to the corresponding binary catalysts. In addition, the turnover frequency for the SCR $DeNO_x$ reaction (10^{-3} to 10^{-2} s^{-1}) is an intermediate between the turnover frequencies for sulfur dioxide oxidation (10^{-6} s^{-1}) and methanol oxidation (10^{0} s^{-1}) at 230°C over supported vanadia catalysts. Therefore, there does not appear to be any evidence that an electronic interaction between the surface vanadia and tungsten oxide species of the ternary catalyst allows redox reactions to proceed more efficiently.

5. Conclusions

Vanadia and tungsten oxide promoted catalysts were prepared on various supports: ceria, zirconia, titania, alumina and silica. Raman spectroscopy was used to confirm the presence and coordination of the surface vanadia and tungsten oxide species on the metal-oxide supports. At low vanadia loadings, the surface vanadia species preferentially exist on the metal oxide support surfaces primarily as isolated tetrahedrally coordinated VO_4 species, each species consisting of a terminal (mono-oxo) V=O bond and three bridging vanadium–oxygen–support (V–O–M) bonds, i.e., $(M–O)_3V^{+5}=O$. At higher vanadia loadings, the isolated $(M–O)_3V^{+5}=O$ surface species tend to polymerize breaking V–O–M bonds and forming V–O–V bridging bonds.

The turnover frequency for sulfur dioxide oxidation over V_2O_5/TiO_2 was low due to the inefficient adsorption of sulfur dioxide (1×10^{-4} molecules of sulfur dioxide oxidized per surface vanadium oxide site per second at 400°C) and independent of surface vanadia coverage suggesting that only one surface vanadia site is required for the oxidation of sulfur dioxide to sulfur trioxide. As the specific metal-oxide support was varied, the sulfur dioxide oxidation activity of the supported vanadia catalysts varied by approximately one order of magnitude (Ce>Zr, Ti>Al>Si) suggesting the importance of the V–O–M bond in the rate determining step of this oxygen insertion reaction. The basicity of the bridging V–O–M oxygen appears to be responsible for influencing the adsorption and subsequent oxidation of the acidic sulfur dioxide molecule on the surface vanadia site. The oxidation activity due to the bare supports was detectable, but is considered insignificant.

The mechanism of sulfur dioxide oxidation over supported vanadia catalysts involves adsorption and coordination of acidic $SO_{2(g)}$ onto the somewhat basic V–O–M oxygen of surface $(M–O)_3V^{+5}=O$ species followed by cleavage of the $V^{+5}–O–SO_2$ bond and

formation of $SO_{3(g)}$. Reduced (V^{+3}) is then reoxidized by dissociatively adsorbed oxygen. The rate of the oxidation reaction is zero-order with respect to oxygen for partial pressures above 1 vol%, first-order in sulfur dioxide and inhibited by sulfur trioxide. The apparent activation energy for sulfur dioxide oxidation over these catalysts was approximately 21 kcal/mol.

One of the primary impediments in the development of low-temperature (e.g., 200–300°C) $DeNO_x$ catalysts is the reaction between ammonia and sulfur trioxide to form ammonium sulfates, which may deposit on the catalyst surface at temperatures below 250°C. In order to design low-temperature SCR catalysts, it is necessary to identify catalysts that can efficiently promote the SCR reaction without significantly increasing the oxidation of sulfur dioxide. Previous studies have found that V_2O_5/TiO_2 catalysts promoted with tungsten oxide showed a dramatic increase in SCR activity in comparison to the unpromoted samples, which is attributed to the increased Brønsted acidity exhibited by these catalysts. The turnover frequency for sulfur dioxide oxidation over WO_3/TiO_2 was an order of magnitude lower than that found for V_2O_5/TiO_2 (i.e., 1×10^{-5} molecules of sulfur dioxide oxidized per surface tungsten oxide site per second at 400°C), and no redox synergism between the surface vanadia and tungsten oxide species was evident for a ternary 1% V_2O_5/7% WO_3/TiO_2 catalyst. This suggests that tungsten oxide is an effective additive for V_2O_5/TiO_2 catalysts at promoting the selective catalytic reduction of nitric oxide, while also exhibiting low activity towards the oxidation of sulfur dioxide to sulfur trioxide.

Acknowledgements

The financial support of the National Science Foundation grant no. CTS-9626893 is gratefully acknowledged.

References

[1] C.D. Cooper, F.C. Alley, Air Pollution Control: A Design Approach, Waveland Press, Prospect Heights, IL, 1994.
[2] H. Bosch, F.J.J.G. Janssen, Catal. Today 2 (1988) 369.
[3] J. Armor, Appl. Catal. B 1 (1992) 221.
[4] N. Ohlms, Catal. Today 16(2) (1993) 247.
[5] A. Urbanek, M. Trela, Catal. Rev.-Sci. Eng. 21(1) (1980) 73.
[6] B. Balzhinimaev, A. Ivanov, O. Lapina, V. Mastikhin, K. Zamaraev, Faraday Discuss. Chem. Soc. 87 (1989) 133.
[7] O. Lapina, V. Mastikhin, A. Shubin, V. Krasilnikov, K. Zamaraev, Prog. NMR Spec. 24 (1992) 457.
[8] J. Svachula, L. Alemany, N. Ferlazzo, P. Forzatti, E. Tronconi, F. Bregani, Ind. Eng. Chem. Res. 32 (1993) 826.
[9] S. Morikawa, H. Yoshida, K. Takahashi, S. Kurita, Chem. Lett. (1981) 251.
[10] S. Morikawa, H. Yoshida, K. Takahashi, S. Kurita, Proceedings of the Eighth International Congress on Catalysis, 1984, p. 661.
[11] N. Sazonova, L. Tsykoza, A. Simakov, G. Barannik, Z. Ismagilov, React. Kinet. Catal. Lett. 52(1) (1994) 101.
[12] M. Imanari, Y. Watanbe, Proceedings of the Eighth International Congress on Catalysis, 1984, p. 841.
[13] M.A. Vuurman, A.M. Hirt, I.E. Wachs, J. Phys. Chem. 95 (1991) 9928.
[14] J.P. Dunn, M.S. Thesis, Lehigh University, Bethlehem, PA, 1995.
[15] G. Deo, I.E. Wachs, J. Haber, Crit. Rev. Surf. Chem. 4 (3/4) (1994) 141; I.E. Wachs, B.M. Weckhuysen, Appl. Catal. A. Gen. 157 (1997) 67.
[16] N. Das, H. Eckert, H. Hu, I.E. Wachs, J.F. Walzer, F.J. Feher, J. Phys. Chem. 97 (1993) 8240.
[17] I.E. Wachs, Catal. Today 27 (1996) 437.
[18] I.E. Wachs, Coll. Surf. A 105 (1995) 143.
[19] F.D. Hardcastle, I.E. Wachs, J. Phys. Chem. 95 (1991) 5031.
[20] W.L. Holstein, C.J. Machiels, J. Catal. 162 (1996) 118.
[21] R.T. Sanderson, J. Chem. Edu. 65(2) (1988) 112.
[22] P. Forzatti, E. Tronconi, A.S. Elmi, G. Busca, Appl. Catal. A (1997).
[23] I.E. Wachs, Thirteenth Award for Excellence in Catalysis Lecture, Catalysis Society of Metropolitan New York, Somerset, NJ, 15 May 1996.
[24] W.S. Kiljstra, N.J. Komen, A. Andreini, E.K. Poels, A. Bliek, Proceedings of the Eleventh International Congress on Catalysis, 1996, p. 951.
[25] J. Le Bars, J.C. Vedrine, A. Auroux, S. Trautmann, M. Baerns, Appl. Catal. A 119 (1994) 341.
[26] M.D. Amiridis, I.E. Wachs, G. Deo, J.M. Jehng, D.S. Kim, J. Catal. 161 (1996) 247.
[27] J.P. Dunn, J.M. Jehng, D.S. Kim, L.E. Briand, H.G. Stenger, I.E. Wachs, J. Phys. Chem. B 102 (1998) 6212.
[28] L. Lietti, P. Forzatti, F. Bregani, Ind. Eng. Chem. Res. 35 (1996) 3884.
[29] N.Y. Topsoe, J. Catal. 128 (1991) 499.
[30] R.A. Rajadhyaksha, F. Knozinger, Appl. Catal. 51 (1989) 81.
[31] J.P. Chen, R.T. Yang, J. Catal. 125 (1990) 411.
[32] I.E. Wachs, G. Deo, B.M. Weckhuysen, A. Andreini, M.A. Vuurman, M. de Boer, M.D. Amiridis, J. Catal. 161 (1996) 211.
[33] M.D. Amiridis, I.E. Wachs, G. Deo, J.M. Jehng, D.S. Kim, J. Catal. 161 (1996) 247.
[34] G. Deo, I.E. Wachs, J. Catal. 146 (1994) 323.